Carboxylated phytosterol derivative-introduced liposomes for skin environment-responsive transdermal drug delivery system

Carboxylated phytosterol derivative-introduced liposomes for skin environment-responsive transdermal drug delivery system

Naoko Yamazaki[a,b], Satoshi Yamakawa[c], Takumi Sugimoto[b], Yuta Yoshizaki[b], Ryoma Teranishi[b], Takaaki Hayashi[b], Aki Kotaka[a], Chiharu Shinde[a], Takayuki Kumei[a], Yasushi Sumida[a], Toru Shimizu[c], Yukihiro Ohashi[c], Eiji Yuba[b,*], Atsushi Harada[b], and Kenji Kono[b]

[a] *Research Institute, Fancl Corporation, 12-13 Kamishinano, Totsuka-ku, Yokohama, Kanagawa, Japan*

[b] *Department of Applied Chemistry, Graduate School of Engineering, Osaka Prefecture University, 1-1 Gakuen-cho, Naka-ku, Sakai, Osaka 599-8531, Japan*

[c] *Cosmetic Ingredients Laboratory, Nippon Fine Chemical Corporation, 1-1, 5-Chome, Umei, Takasago, Hyogo 676-0074, Japan*

***Corresponding author: Eiji Yuba**

Department of Applied Chemistry, Graduate School of Engineering,

Osaka Prefecture University, 1-1 Gakuen-cho, Naka-ku, Sakai, Osaka 599-8531, Japan

Tel.: +81-722-54-9913; Fax: +81-722-54-9330; yuba@chem.osakafu-u.ac.jp

Abstract

Transdermal drug delivery systems are a key technology for skin-related diseases and for cosmetics development. The delivery of active ingredients to an appropriate site or target cells can greatly improve the efficacy of medical and cosmetic agents. For this study, liposome-based transdermal delivery systems were developed using pH-responsive phytosterol derivatives as liposome components. Succinylated phytosterol (Suc-PS) and 2-carboxy-cyclohexane-1-carboxylated phytosterol (CHex-PS) were synthesized by esterification of hydroxy groups of phytosterol. Modification of phytosterol derivatives on 1,2-dimyristoyl-*sn*-glycero-3-phosphocholine (DMPC) liposomes was confirmed by negatively zeta potentials at alkaline pH and the change of zeta potentials with decreasing pH. In response to acidic pH and temperatures higher than body temperature, Suc-PS-containing and CHex-PS-containing liposomes exhibited content release at intracellular acidic compartments of the melanocytes at the basement membrane of the skin. Phytosterol-derivative-containing liposomes were taken up by murine melanoma-derived B16-F10 cells. These liposomes delivered their contents into endosomes and cytosol of B16-F10 cells. Furthermore, phytosterol-derivative-containing liposomes penetrated the 3D skin models and reached the basement membrane. Results show that pH-responsive

phytosterol-derivative-containing DMPC liposomes are promising for use in transdermal medical or cosmetic agent delivery to melanocytes.

Keywords:

liposome / phytosterol / pH-sensitive / transdermal delivery / cosmetics

Introduction

Transdermal drug delivery has been regarded as an alternative to intravenous or oral drug administration. The delivery of cosmetic agents by transdermal routes is particularly attractive in the cosmetic field to improve skin condition for beauty care or anti-aging (Cevc et al., 1996). To achieve transdermal drug delivery, active agents such as antioxidants or UV-protective compounds must penetrate into skin and be delivered to target cells such as melanocytes existing in the basement membrane of skin (Shindo et al., 1993). However, penetration of these agents into skin is difficult because the skin surface is covered with the stratum corneum, which comprises ordered keratinocytes and intercellular lipids (Dayan, 2005). To improve the skin penetration of active agents, various transdermal drug delivery systems (TDDS) have been studied using physical techniques (electroporation, iontophoresis, and microneedles) and nanocarrier-based techniques (polymeric micelle, liposome, nanogel, etc.) (Barry et al., 1987; Cevc et al., 2002; Damme et al., 2009; Elsabahy et al., 2012; Junginger et al., 1991; Lasch et al., 1996; Shah et al., 2012; Verma et al., 2003; Yamazaki et al., 2016). Among them, liposome-based systems have been regarded as attractive TDDS because liposomes are composed mainly of phospholipids, which are compounds found in skin, able to encapsulate both hydrophilic and hydrophobic active agents. They can be functionalized easily by the introduction of functional materials.

The skin surface is weakly acidic and about 30 °C, whereas the deep site of skin is 35–37 °C, with neutral pH (Abe et al., 1980; Behne et al., 2002; Fox et al., 1973; Harrison et al., 1986). Moreover, after internalization to melanocytes in the basement membrane, liposomes are exposed to acidic environments inside of cells (endosome and lysosome) at 35–37 °C. Considering such environmental differences that occur with skin penetration, the introduction of stimuli (pH and temperature)-responsive functions is necessary to produce more efficient liposome-based TDDS.

Generally, two strategies are used for the introduction of stimuli-responsive functions to liposomes: the modification of liposomes with stimuli-sensitive polymers or the use of stimuli-sensitive lipids as liposome components. For polymer modification, poly(carboxylic acid)s such as poly(acrylic acid) derivatives, carboxylated poly(glycidol)s or polysaccharides are used for pH-sensitization of liposomes (Kono et al., 1994; Qiu et al., 2014; Seki and Tirrell, 1984; Yuba et al., 2014). Liposomes modified with poly(carboxylic acid)s exhibited content release in response to the pH decrease. These hydrophilic polymers take a random coil structure at neutral pH, but they become hydrophobic and form a globular structure after protonation of carboxy groups at acidic pH, which strongly destabilizes the liposomal membrane via hydrophobic interaction (Kono et al., 1994; Murthy et al., 1999; Yuba et al., 2011). However, polymers generally have molecular

weight distribution. Therefore, precise control of responsiveness to complex external environments such as skin is difficult.

As another strategy for the preparation of pH-sensitive liposomes, the mixture of non-bilayer forming lipids such as dioleoylphosphatidylethanolamine (DOPE) and pH-sensitive amphiphiles such as cholesteryl hemisuccinate (CHEMS), ester of cholesterol and succinic acid, has been reported (Hafez et al., 2000; Slepushkin et al., 1997). The mixture of DOPE and CHEMS forms a bilayer at neutral pH by hydration of carboxylates of CHEMS, whereas the mixture takes a hexagonal II phase derived from DOPE after protonation of carboxylates of CHEMS at acidic pH, engendering the induction of membrane fusion. CHEMS-based pH-sensitive liposomes are useful as intracellular delivery systems for drugs of various kinds, responding to weakly acidic pH in endosomes. However, the use of non-bilayer forming lipid (DOPE) has shortcomings from the perspective of liposome stability. In addition, plant-derived sterol, phytosterol, has gained much attention as a crude material for cosmetic additives as alternatives for cholesterol, which is derived from animal organs (Pola Chemical Industry Inc., 2007; The Procter & Gamble Company, 2005; Teshigawara et al., 2009). Although the introduction of phytosterol to liposomes or cosmetics has increased the colloidal stability of liposomes

(Pola Chemical Industry Inc., 2007; The Procter & Gamble Company, 2005; Muramatsu et al., 1994), these liposomes or formulations have no stimuli-responsive property as TDDS.

For this study, the development of skin environment-responsive liposome-based TDDS that can promote the penetration of liposomes to basement membrane and which can achieve controlled release of active ingredients inside of melanocytes was attempted. For pH-sensitization of liposomes, phytosterol derivatives having pH-sensitive function were designed (Fig. 1). Esters of phytosterol with succinic acid or cyclohexanedicarboxylic acid were synthesized via reaction of phytosterol with corresponding dicarboxylic acid anhydrides. Phytosterol derivatives were introduced to 1,2-dimyristoyl-*sn*-glycero-3-phosphocholine (DMPC)-based liposome, which is a bilayer-forming lipid with a gel-to-liquid crystalline transition temperature of 23–24 °C (Needham et al., 1988; Taylor et al., 1995). Therefore, liposome composed of phytosterol derivatives/DMPC is expected to respond to both weakly acidic pH at skin surface or endo/lysosome in melanocytes and temperature during skin penetration (25–37 °C). This study was conducted to characterize phytosterol derivatives, pH-/temperature-sensitivity of phytosterol derivative-introduced liposomes, interaction with melanocytes, and penetration of skin models.

Materials and methods

Materials

Succinic anhydride and 1,2-cyclohexanedicarboxylic acid anhydride were obtained from New Japan Chemical Co., Ltd. (Tokyo, Japan). DMPC was obtained from NOF Corp. (Tokyo, Japan). Calcein was from Sigma-Aldrich Corp. (St. Louis, MO, USA). Lissamine rhodamine B-sulfonylphosphatidylethanolamine (Rh-PE) was purchased from Avanti Polar Lipids Inc. (Birmingham, AL, USA). Triton X-100 was obtained from Tokyo Chemical Industry Co. Ltd. (Tokyo, Japan). Phytosterol was provided from TAMA Biochemical Co., Ltd. (Tokyo, Japan). Its composition was ascertained using gas chromatography as β-sitosterol 46%, campesterol 25%, stigmasterol 21%, brassicasterol 3%, and other sterols 5%.

Cell culture

B16-F10 melanoma cells obtained from Tohoku University (Sendai, Japan) were grown at 37 °C in DMEM containing 10% FBS and antibiotics in a humidified atmosphere containing 5% CO_2.

Synthesis of phytosterol derivatives

Phytosterol derivatives were synthesized by the reaction of phytosterol (PS) with various dicarboxylic acid anhydrides. For succinylated phytosterol (Suc-PS), phytosterol (73.6 g, 0.18 mol) and succinic anhydride (20.0 g, 0.20 mol) were dissolved in 190 mL of toluene. Then the solution was stirred with reflux for 8 h under N_2 atmosphere. Subsequently, methyl ethyl ketone (12.6 mL) and purified water (65.0 mL) were added to the reaction solution, which was then kept at 60 °C for 1 h with stirring. Then, the reaction mixture was washed with purified water until the pH of aqueous phase became neutral. Organic phase was concentrated under vacuum and Suc-PS was recrystallized from heptane as a white powder. The yield was 65.4 g (71.4%). 2-Carboxy-cyclohexane-1-carboxylated phytosterol (CHex-PS) was synthesized using the same procedure, except that 1,2-cyclohexanedicarboxylic acid anhydrides were used. The yield of CHex-PS was 54.3 g (59.5%). Phytosterol derivatives were characterized using ^{1}H NMR, ^{13}C NMR (Figs. S1–S6, JNM-AL-300; JEOL), and FT-IR (Figs. S7–S9, FTIR-8400S; Shimadzu).

Preparation of calcein-loaded liposomes

The given amounts of chloroform/methanol solution of DMPC and phytosterol derivatives were added to a flask (38 μmol, DMPC/phytosterol derivative = 6/4, mol/mol).

Then the solvent was evaporated. After the obtained thin film was dried further overnight under vacuum, it was dispersed in 2 mL of aqueous calcein solution (63 mM, pH 7.4) at 90 °C to peel the thin film from the flask completely. The liposome suspension was extruded through a polycarbonate membrane with 100 nm pore diameter at 50 °C, which is a much higher temperature than the liquid-gel crystalline temperature of DMPC (23 °C). The free calcein was removed using a column (Sephadex G-50; GE Healthcare UK Ltd., Buckinghamshire, UK) at 4 °C in a 10 mM phosphate and 137 mM NaCl solution at pH 9.0. The lipid concentration was determined using Test-Wako-C (Wako Pure Chemical Industries Ltd., Osaka, Japan). The liposome size and zeta potential were evaluated using dynamic light scattering (ELS-8000 and ELS-Z 1000; Otsuka Electronics Co. Ltd., Tokyo, Japan) in Dulbecco's phosphate buffered saline (PBS) with various pH at 25 °C. Transmission electron microscopy (TEM, JEM-2000FEX II; JEOL Ltd., Tokyo, Japan) with carbon-coated copper grids was used for analysis of the liposomes stained with phosphotungstic acid solution.

Calcein release from liposomes

Liposome suspension was added to PBS (4.0 mL) at various pH (pH 4.0–7.4) and temperatures (25–55 °C). The final concentrations of lipid and calcein were 0.02 mM and

0.05 μM, respectively. Calcein fluorescence at 520 nm with excitation at 490 nm was measured using spectrophotofluorimetry (FP-6200, FP-6500, FP-8500S, FP-8600S; Jasco Corp., Spectra Max Gemini EM; Molecular Devices Corp., MT, USA). The incubation time for fluorescence measurements was set to 30 min for analysis of pH-dependence and 10 min for analysis of temperature dependence because calcein fluorescence tended to decrease at high temperatures. The percent release of calcein from liposome was defined as

$$\%\text{Release} = (F - F_0)/(F_{100} - F_0) \times 100 ,$$

where F_0 and F respectively denote the initial and intermediary fluorescence intensities of the liposome suspension at 5 °C. F_{100} is the fluorescence intensity of the liposome suspension after the addition of Triton X-100 (final concentration, 0.2 wt%).

Confocal laser scanning microscopic observation

Liposomes containing Rh-PE were prepared as described above, except that a mixture of DMPC and phytosterol derivatives containing 0.2 mol% of Rh-PE was dispersed in the calcein solution. B16-F10 cells (2.0×10^5 cells) cultured for 24 h in 35 mm glass bottom dishes were washed with PBS containing Ca^{2+} and Mg^{2+} (PBS(+)). Then

they were incubated in serum-free DMEM (1 mL). The Rh-PE-labeled and calcein-loaded liposomes (0.4 mM lipid concentration, 1 mL) were added gently to the cells and were incubated for 3 h at 37 °C. After the cells were washed with PBS(+), they were observed using confocal laser scanning microscopy (LSM 5 Exciter; Carl Zeiss Inc., Oberkochen, Germany).

Flow cytometry

After the B16-F10 cells (5.0×10^4 cells) cultured for 24 h in 24-well plates were washed with PBS(+), they were incubated in serum-free DMEM (0.5 mL). The Rh-PE-labeled and calcein-loaded liposomes (1.0 mM lipid concentration, 0.5 mL) were added gently to the cells and were incubated for 3 h at 37 °C. The cells were washed with PBS(+). The fluorescence intensity of cells detached by trypsin was ascertained using flow cytometric analysis (CytoFlex; Beckman Coulter Inc., Fullerton, CA, USA).

Penetration behavior of liposomes in skin models

3D skin models (LabCyte EPI-Model; Japan Tissue Engineering Co., Ltd., Aichi, Japan) were used to evaluate liposome penetration. 3D skin models were treated with 0.2 mol% Rh-PE-labeled liposomes containing calcein (1 mM lipid and 25.2 μM calcein

concentrations) for 24 h in PBS. After removal of the supernatant, 3D skin models were frozen immediately after embedding in Tissue-Tek O.C.T. Compound (Sakura Finetek Japan Co., Ltd., Tokyo, Japan). Skin models were sectioned into 10 μm slices using a cryomicrotome (CM1520; Leica) and were mounted on glass slides. Confocal laser scanning microscopic (CLSM) analysis of these slides was conducted using an LSM 5 Exciter.

Statistical analysis

Student's *t*–test was performed in the statistical evaluation of the results (Figs. 5, 6 and 8).

Results and Discussion

Characterization of phytosterol derivatives

Phytosterol derivatives of two kinds, succinylated phytosterol (Suc-PS) and 2-carboxy-cyclohexane-1-carboxylated phytosterol (CHex-PS), were synthesized by reaction of phytosterol with various dicarboxylic acid anhydrides according to an earlier report of the literature (Sakaguchi et al., 2008) (Fig. 2). Because the phytosterol used for this study is a mixture of various sterol derivatives such as β-sitosterol, stigmasterol, campesterol, brassicasterol, and other sterols as described in *Materials*, the introduction of the ester groups to phytosterol was evaluated through comparison of ^{1}H NMR and ^{13}C NMR spectra for the parent phytosterol (Figs. S1 and S4) and for phytosterol derivatives (Figs. S2, S3, S5, and S6). The existence of new peaks corresponding to each dicarboxylic acid ester group and the shift of peak corresponding to proton next to sterol hydroxy group (from 3.5 ppm to 4.6 ppm in ^{1}H NMR and from 71.7 ppm to 74.5 ppm in ^{13}C NMR) confirmed the complete conversion of sterol hydroxy groups to carboxylic acid ester groups. Introduction of the ester groups was confirmed further by the existence of asymmetric vibration bands corresponding C=O of ester group at around 1700 cm^{-1} in FT-IR spectra (Figs. S8 and S9) compared with the parent phytosterol (Fig. S7).

Preparation of phytosterol derivative-containing liposomes

Phytosterol derivative-containing liposomes were prepared by the dispersion of mixed thin film composed of DMPC and phytosterol derivatives. Liposome suspension was extruded further through a polycarbonate membrane with pore size of 100 nm and was purified using a gel permeation chromatography (GPC) column. In the absence of phytosterol derivatives, the size distribution of DMPC liposomes was too broad and was unstable under experimental conditions (data not shown). In contrast, phytosterol derivative-containing DMPC liposomes showed a narrow size distribution (PDI < 0.20) and size of 100 nm, which corresponds to the pore size diameter during extrusion (Table 1). Reportedly, the introduction of soybean-derived sterol or cholesterol increased the stability of liposomes by adjusting membrane fluidity (Muramatsu et al., 1994). Therefore, the introduction of phytosterol or phytosterol derivatives to DMPC liposomes might also increase the liposomal membrane stability. Figure 3 depicts TEM analysis of phytosterol derivative-containing DMPC liposomes. Irrespective of the structure of phytosterol derivatives, 100–200 nm vesicular particles were observed, which is typical for the liposome morphology (Di Marzio et al., 2008). These results indicate that the mixture of phytosterol or phytosterol derivative and DMPC can take a stable lamellar phase and can form stable liposomes.

To confirm the modification of carboxylated phytosterols onto the liposome, zeta potentials of liposome at various pH were evaluated (Fig. 4). Parent phytosterol-containing liposomes (PS liposomes) showed almost neutral zeta potentials at pH 5–9, indicating that the polar head groups of phytosterol and DMPC did not change the charged state in this pH region. In contrast, phytosterol derivative-containing DMPC liposomes showed negative zeta potentials at pH 9 (-25 – 30 mV). Zeta potentials of these liposomes increased concomitantly with decreasing pH. They became almost neutral at pH 5. These results indicate that deprotonated carboxy groups of phytosterol derivatives were presented onto liposomal membrane at alkaline pH and that these carboxy groups were protonated with decreasing pH. The same tendency was described for DMPC/CHEMS liposomes in earlier reports of the literature (Di Marzio et al., 2008). The zeta potentials of DMPC/CHEMS liposomes in 10 mM Hepes buffer were -82 mV at pH 7.4 and -35 mV at pH 5.5, whereas the zeta potentials of DMPC/cholesterol liposomes changed only slightly at pH 7.4 (-23 mV) and pH 5.5 (-18 mV). Such charge conversion during alkaline pH to weakly acidic pH in phytosterol derivative-containing liposomes might alter the interaction of phytosterol derivatives with lipid membranes. Compared with Suc-PS-containing liposomes, CHex-PS-containing liposomes showed higher zeta potentials at the neutral and weakly acidic pH region, although zeta potentials of these liposomes were almost identical at pH 9.

Protonation of carboxy groups was affected strongly by the chemical structure next to the carboxy group. The more hydrophobic structure promotes the protonation of carboxy group, as described for poly(glycidol) derivatives having various side chain structures (Sakaguchi et al., 2008). CHex-PS has a more hydrophobic cyclohexane structure than that of Suc-PS. Therefore, the protonation of carboxy groups in CHex-PS might be promoted compared with Suc-PS. Although we were unable to ascertain the pKa values of PS derivatives by titration because of their insolubility in water and interruption by turbidity, the hydrophobic structure of CHex-PS might increase the protonation degree of carboxy group on liposome surface compared with Suc-PS, leading to the increased pKa value.

Stimuli-sensitive properties of phytosterol derivative-containing liposomes

Zeta potentials of phytosterol derivative-containing DMPC liposomes changed depending on the environmental pH (Figure 4). Therefore, pH-responsive drug release behaviors of these liposomes were evaluated using fluorescence dye calcein-loaded liposomes. Figure 5 depicts the pH-dependence of calcein release from liposomes after 30 min incubation at 25 °C and 35 °C: the latter corresponds to the temperature at the deep site of skin (Fox et al., 1973). Under the temperatures and pH region used for experiments, PS liposome showed no calcein release, which indicates that this liposome is quite stable

under these conditions. In contrast, phytosterol derivative-containing liposomes exhibited content release at low pH, which is the same result as that obtained in the case of DMPC/CHEMS liposomes (Di Marzio et al., 2008). At neutral pH, carboxylates on the liposome surface might suppress the destabilization of liposomal membrane via electrostatic repulsion. However, protonated carboxy groups at low pH might form hydrogen bonds with phosphate groups of DMPC and might destabilize the lipid membrane via hydrophobic interaction (Kono et al., 1994; Sakaguchi et al., 2008; Seki and Tirrell, 1984). The carboxylic acid ester structure affected the pH at which the content release occurred. At 35 °C, Suc-PS liposomes induced content release below pH 5.5, whereas CHex-PS liposomes induced content release below pH 7.0 (Figure 5b). The more hydrophobic structures of CHex-PS promoted protonation of carboxy groups and interaction with lipid membrane, resulting in content release at higher pH than that of Suc-PS as reported earlier in the literature (Sakaguchi et al., 2008). Compared with the case at 25 °C (Figure 5a), phytosterol derivative-containing liposomes exhibited high release properties at 35 °C (Figure 5b). This result reflects that the high temperature might increase the fluidity of liposomal membrane and promote drug release at low pH.

To verify the temperature-sensitive drug release properties of liposomes, calcein release from liposomes was examined at various temperatures (Figure 6). At neutral pH, no

liposome showed content release from 25 °C to 55 °C after 10 min incubation. At pH 7.4, most carboxy groups on Suc-PS or CHex-PS liposome surface are deprotonated, which suppresses interaction with lipid membrane by electrostatic repulsion. Therefore, no release was observed for any PS derivative-containing liposomes at least during 10 min incubation. At pH 5.0, both PS liposomes and Suc-PS liposomes retained their contents at all examined temperatures. In contrast, CHex-PS liposomes showed greater than 50% content release at temperatures higher than 30 °C. These results indicate that CHex-PS liposomes can efficiently destabilize liposomal membrane within 10 min at low pH and high temperatures. Consequently, CHex-PS liposome retained their contents at neutral pH and at any temperatures, while inducing content release at low pH and 35 °C, which corresponds to skin temperature and intracellular acidic compartments such as lysosomes (Fox et al., 1973; Mukherjee et al., 1997). Therefore, CHex-PS liposome is anticipated for use as a skin environment-responsive liposome.

Interaction of phytosterol derivative-containing liposomes with cells

To investigate the function of phytosterol derivative-containing liposomes as intracellular delivery vehicles, intracellular distributions of liposomes and contents were observed using CLSM. Calcein-loaded and rhodamine lipid-labeled liposomes were

applied to murine melanoma-derived B16F10 cells, a melanocyte model. In the case of PS liposome-treated cells, red and green fluorescent dots were observed from the periphery of cells and near the nucleus (Figure 7a). These results indicate that PS liposomes were taken up by cells via endocytosis and were trapped in early endosomes (periphery) and/or late endosomes/lysosomes (near nucleus) (Straubinger et al., 1983; Düzgünes and Nir 1999; Huth et al., 2006). Green fluorescence near nucleus was stronger than the cellular periphery. Considering that calcein fluorescence is quenched when calcein molecules are retained inside of liposomes at high concentrations (Allen and Cleland, 1980; Shimanouchi et al., 2009), green fluorescent dots near the nucleus indicate the release of calcein molecules from liposomes. Actually, PS liposomes have no pH-responsive properties at 37 °C (Figures 5 and 6); the calcein and Rh fluorescence near the nucleus were almost overlapped. Therefore, PS liposomes might be degraded by lysosomes; the leakage of calcein molecules inside of lysosome was observed as green fluorescent dots near the nucleus. In the case of Suc-PS liposome-treated cells, red fluorescent dots were observed inside the cells but green dots were not (Figure 7b). The pH-sensitivity of Suc-PS liposomes at weakly acidic pH is low (Figures 5b and 6b). Therefore, Suc-PS might be unable to induce content release within cells. Furthermore, rhodamine fluorescence of Suc-PS liposome-treated cells was lower than that of PS liposome-treated cells. The

fluorescence intensity of liposome-treated cells was found using flow cytometric analysis (Figures S10 and 8). Compared with PS liposome-treated cells, Suc-PS liposome-treated cells showed low calcein and rhodamine fluorescence intensity, which is consistent with the results of CLSM images. Negatively charged carboxylates on Suc-PS liposome might suppress the interaction of liposome with cells. The rhodamine fluorescence of CHex-PS liposome-treated cells was also lower than that of PS liposomes (Figures 7c and 8a). In the case of CHex-PS liposome-treated cells, both red and green fluorescent dots were observed within cells. Calcein fluorescence was observed not only from near the nucleus but also from the cellular periphery, unlike the case of PS liposomes. Furthermore, not only yellow dots, denoting the colocalization of liposome and released calcein molecules in endo/lysosomes; green dots were also observed, indicating that calcein molecules might escape from endo/lysosomes. Although cellular association of CHex-PS liposomes was low compared with PS liposomes, CHex-PS liposomes might destabilize and release calcein responding to acidic pH and cultural temperature (37 °C), as presented in Figures 5b and 6b, after internalization to early endosomes and late endosomes/lysosomes. CHex-PS became hydrophobic at low pH and might further interact with endosomal membrane, which promoted the escape of calcein molecules from endo/lysosomes. Such an intracellular release property of CHex-PS liposomes was confirmed further by the

calculation of calcein fluorescence per rhodamine fluorescence, which indicates the release efficacy of calcein per endocytosed liposomes. As portrayed in Figure 8b, CHex-PS liposomes showed a three-times-higher calcein/rhodamine ratio than those of PS liposome and Suc-PS liposome. Therefore, CHex-PS liposomes are efficient intracellular delivery carriers responding to both low pH and skin temperature.

Transdermal delivery

Finally, transdermal delivery of liposome and contents were investigated using 3D skin models (LabCyte EPI Model), which are generally used models for drug penetration experiments in the cosmetic field instead of animal-derived skins (Hikima et al., 2012; Yamazaki et al., 2017). Three-dimensional skin models were incubated with calcein-loaded and Rh-PE-labeled liposomes for 24 h. After the skin models were sectioned, their cross-sections were observed using CLSM (Figure 9). Strong green and red fluorescence was observed from the surface of liposome-treated skin models, which corresponds to the stratum corneum. This result indicates that most liposomes absorbed to the stratum corneum even after 24 h-incubation. Weak green and red fluorescence was detected from underlayers of the stratum corneum. Some fluorescence reached the basement membrane, as indicated by arrowheads. Especially, Suc-PS liposome and CHex-PS liposome exhibited higher

fluorescence intensity than that of PS liposomes at the basement membrane. Moreover, both lipid-derived and calcein-derived fluorescence were detected from the same location in the basement membrane. These results suggest two possibilities: after destabilization of liposomes in the stratum corneum, calcein and Rh-PE reached the basement membrane independently, or calcein-loaded liposomes reached the basement membrane. Controversial reports of transdermal penetration of liposomes have failed to clarify whether liposomes retain their structure, or not (Dreier et al., 2016; Wang et al., 2013; Park et al., 2013). In our case, considering that the free calcein solution was unable to penetrate and reach the basement membrane under the same conditions (data not shown) and considering that these liposomes showed lower interaction with cells than that of PS liposome (Figure 8a), one might infer that phytosterol derivatives enhance the penetration of liposomes by affecting the intercellular lipids of skin models. Further investigation must be undertaken to elucidate the penetration mechanisms of phytosterol derivative-containing liposomes from the stratum corneum to the basement membrane. Phytosterol derivative-containing liposomes, especially CHex-PS liposomes, might be taken up by melanocytes in the basement membrane and might release their contents into cytosol in response to body temperature and low pH in endo/lysosomes of melanocytes. Now we are conducting safety assessments of these liposomes for application to cosmetics. At least, the treatment of carboxylated

sterol-containing liposomes did not affect the morphology of cell and 3D skin model under experimental conditions (Figures 7 and 9). Therefore, we believe that carboxylated sterol-containing liposomes are safe and that they produce no skin irritation.

Conclusion

For this study, pH-responsive phytosterol esters were newly synthesized. Carboxylated phytosterol-containing liposomes triggered content release responding to acidic pH and temperatures higher than body temperature, which corresponds to a skin environment or intracellular acidic compartments of melanocytes. In addition, these liposomes achieved penetration into skin model basement membranes. Therefore, these liposomes are demonstrated as useful for the delivery of active ingredients to melanocytes existing in deep skin tissues, which provides highly protective effects against the production of melanin and freckles.

Acknowledgments

This work was supported by a Grant-in-aid for Scientific Research from the Ministry of Education, Culture, Sports, Science, and Technology in Japan (26242049).

Declaration of interest

The authors have no conflict of interest, financial or otherwise, related to this study.

References

Abe T, Mayuzumi J, Kikuchi N et al. (1980). Seasonal variations in skin temperature, skin pH, evaporative water loss and skin surface lipid values on human skin. Chem Pharm Bull 28:387–92.

Allen TM, Cleland LG. (1980). Serum-induced leakage of liposome contents. Biochim Biophys Acta 597:418–26.

Barry BW. (1987). Mode of action of penetration enhancers in human skin. J Control Release 6:85–97.

Behne MJ, Meyer JW, Hanson KM et al. (2002). NHE1 regulates the stratum corneum permeability barrier homeostasis microenvironment acidification assessed with fluorescence lifetime imaging. J Biol Chem 277:47399–406.

Cevc G, Blume G, Schätzleina A et al. (1996). The skin: a pathway for systemic treatment with patches and lipid-based agent carriers. Adv Drug Deliver Rev 1:349–78.

Cevc G, Schätzlein A, Richardsen H et al. (2002). Ultradeformable lipid vesicles can penetrate the skin and other semi-permeable barriers unfragmented. Evidence from double label CLSM experiments and direct size measurements. Biochim Biophys Acta 1564:21–30.

Damme PV, Oosterhuis-Kafeja F, Wielen MV et al. (2009). Safety and efficacy of a novel microneedle device for dose sparing intradermal influenza vaccination in healthy adults. Vaccine 14:454–9.

Dayan N. (2005). Pathways for skin penetration. Cosmet Toiletries 120:67-76.

Di Marzio L, Marianecci C, Cinque B et al. (2008). pH-sensitive non-phospholipid vesicle and macrophage-like cells: Binding, uptake and endocytotic pathway. Biochim Biophys Acta 1778: 2749–56.

Dreier J, Sørensen JA, Brewer JR. (2016). Superresolution and fluorescence dynamics evidence reveal that intact liposomes do not cross the human skin barrier. PLoS One 11:e0146514.

Düzgünes N, Nir S. (1999). Mechanisms and kinetics of liposome-cell interactions. Adv Drug Deliv Rev 40:3–18.

Elsabahy M, Wooley KL. (2012). Design of polymeric nanoparticles for biomedical delivery applications. Chem Soc Rev 41:2545–61.

Fox RH, Solman AJ, Isaacs R et al. (1973). A new method for monitoring deep body temperature from the skin surface. Clin Sci 44:81–6.

Hafez IM, Ansell S, Cullis PR. (2000). Tunable pH-sensitive liposomes composed of mixtures of cationic and anionic lipids. Biophys J 79:1438–46.

Harrison DK, Spence VA, Beck JS et al. (1986). pH changes in the dermis during the course of the tuberculin skin test. Immunology 59:497–501.

Hikima T, Kaneda N, Matsuo K et al. (2012). Prediction of percutaneous absorption in human using three-dimensional human cultured epidermis LabCyte EPI-MODEL. Biol Pharm Bull 35:362–8.

Huth US, Schubert R, Peschka-Süss R. (2006). Investigating the uptake and intracellular fate of pH-sensitive liposomes by flow cytometry and spectral bio-imaging. J Control Release 110:490–504.

Junginger HE, Hofland HE, Bouwstra JK. (1991). Liposomes and niosomes: interaction with human skin. Cosmet Toiletries 106:45–50.

Kono K, Zenitani K, Takagishi T. (1994). Novel pH-sensitive liposomes: liposomes bearing a poly(ethylene glycol) derivative with carboxyl groups. Biochim Biophys Acta 1193:1–9.

Lasch J, Laub R, Wohlrab W. (1996). How deep do intact liposomes penetrate into human skin? J Control Release 38:267–74.

Mukherjee S, Ghosh RN, Maxfield FR. (1997). Endocytosis. Physiol Rev 77:759–803.

Muramatsu K, Maitani Y, Machida Y et al. (1994). Effect of soybean-derived sterol and its glucoside mixtures on the stability of dipalmitoylphosphatidylcholine and dipalmitoylphosphatidylcholine/cholesterol liposomes. Int J Pharm 107:1–8.

Murthy N, Robichaud JR, Tirrell DA et al. (1999). The design and synthesis of polymers for eukaryotic membrane disruption. J Control Release 61:137–43.

Needham D, Evans E. (1998). Structure and mechanical properties of giant lipid (DMPC) vesicle bilayers from 20 °C below to 10 °C above the liquid crystal-crystalline phase transition at 24 °C. Biochemistry 27:8261–9.

Park SI, Lee EO, Yang HM et al. (2013). Polymer-hybridized liposomes of poly(amino acid) derivatives as transepidermal carriers. Colloids Surf B Biointerfaces 110:333–8.

Pola Chemical Industries Inc., 2007. *Skin external preparation in the form of water-in-oil emulsion comprising ceramide*. European patent application 2088986 A1. 2009-08-19.

The Procter & Gamble Company, 2005. *Regulation of mammalian keratinous tissue using N-acyl amino acid compositions*. International Patent application 011627 A2. 2005-02-10.

Qiu L, Li Z, Qiao M et al. (2014). Self-assembled pH-responsive hyaluronic acid–*g*-poly(L-histidine) copolymer micelles for targeted intracellular delivery of doxorubicin. Acta Biomater 10:2024–35.

Sakaguchi N, Kojima C, Harada et al. (2008). Preparation of pH-sensitive poly(glycidol) derivatives with varying hydrophobicities: their ability to sensitize stable liposomes to pH. Bioconjug Chem 19:1040–8.

Seki K, Tirrell DA. (1984). pH-Dependent complexation of poly(acrylic acid) derivatives with phospholipid vesicle membrane. Macromolecules 17:1692–8.

Shah PP, Desai PR, Patel AR et al. (2012). Skin permeating nanogel for the cutaneous co-delivery of two anti-inflammatory drugs. Biomaterials 33:1607–17.

Shimanouchi T, Ishii H, Yoshimoto N et al. (2009). Calcein permeation across phosphatidylcholine bilayer membrane: effects of membrane fluidity, liposome size, and immobilization. Colloids Surf B Biointerfaces 73:156–60.

Shindo Y, Witt E, Han D et al. (1993). Antioxidant defense mechanisms in murine epidermis and dermis and their responses to ultraviolet light. J Invest Dermatol 100:260–5.

Slepushkin VA, Simões S, Dazin P et al. (1997). Sterically stabilized pH-sensitive liposomes intracellular delivery of aqueous contents and prolonged circulation in vivo. J Bio Chem 272:2382–8.

Straubinger RM, Hong K, Friend DS et al. (1983). Endocytosis of liposomes and intracellular fate of encapsulated molecules: encounter with a low pH compartment after internalization in coated vesicles. Cell 32:1069–79.

Taylor KMG, Morris RM. (1995). Thermal analysis of phase transition behaviour in liposomes. Thermochim Acta 248:289–301.

Teshigawara T, Miyahara R, Fukuhara T et al. (2009). Development of novel cosmetic base using sterol surfactant. II. Solubilizing of sparingly soluble ultraviolet ray absorbers. J Oleo Sci 58:27–36.

Verma DD, Verma S, Blume G et al. (2003). Liposomes increase skin penetration of entrapped and non-entrapped hydrophilic substances into human skin: a skin penetration and confocal laser scanning microscopy study. Eur J Immunol 55:271–7.

Wang Y, Su W, Li Q et al. (2013). Preparation and evaluation of lidocaine hydrochloride-loaded TAT-conjugated polymeric liposomes for transdermal delivery. Int J Pharm 441:748–56.

Yamazaki N, Kumei K, Shinde C et al. (2016). Research on membrane-fluidity and stratum corneum penetration of liposomes made of phospholipid with different acyl groups. J Soc Cosmet Chem Jpn 50:25–32.

Yamazaki N, Sugimoto T, Fukushima M et al. (2017). Dual-stimuli responsive liposomes using pH- and temperature-sensitive polymers for controlled transdermal delivery. Polym Chem 8:1507–18.

Yuba E, Harada A, Sakanishi Y et al. (2011). Carboxylated hyperbranched poly(glycidol)s for preparation of pH-sensitive liposomes. J Control Release 149:72–80.

Yuba E, Tajima N, Yoshizaki Y et al. (2014). Dextran derivative-based pH-sensitive liposomes for cancer immunotherapy. Biomaterials 35:3091–101.

Figures

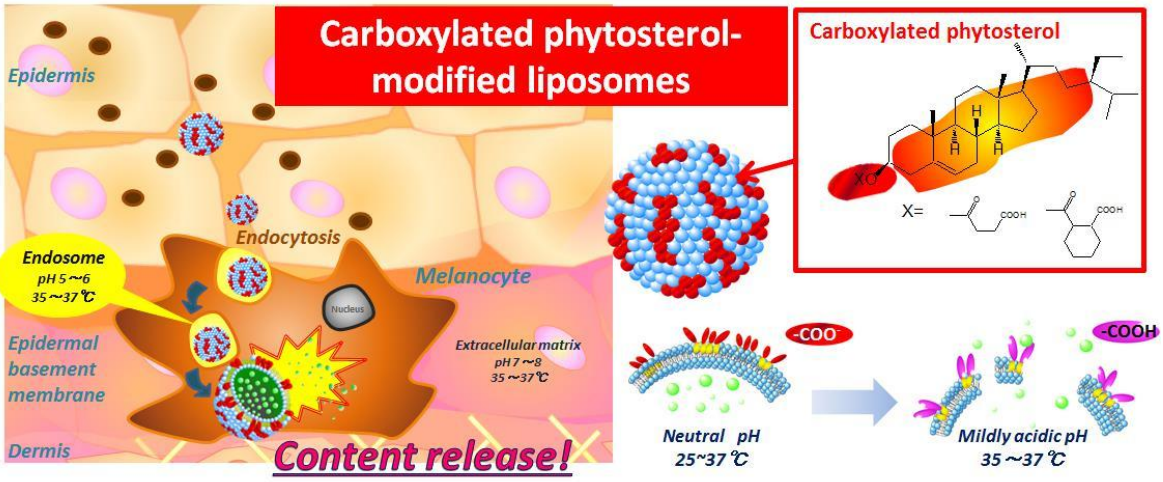

Figure 1. Phytosterol derivative-introduced liposomes for transdermal drug delivery that respond to skin temperature and acidic pH of endosome lumen of melanocytes at the basement membrane.

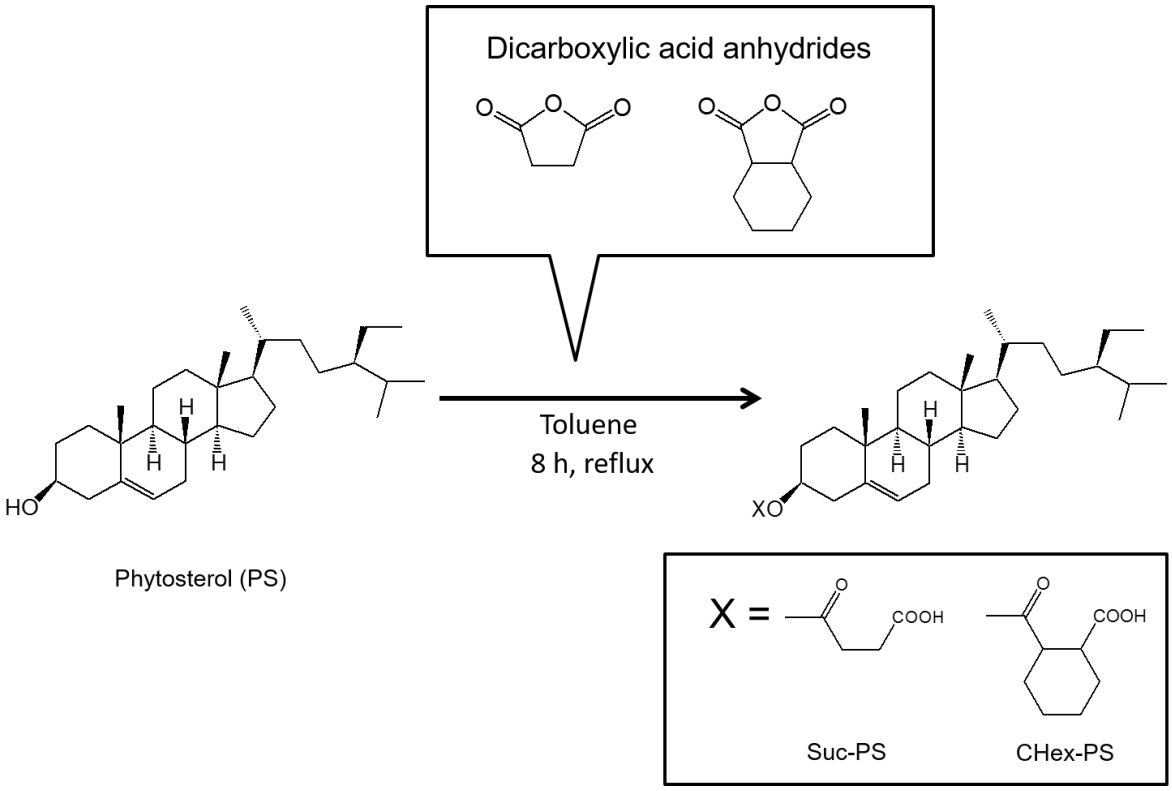

Figure 2. Synthesis of phytosterol derivatives.

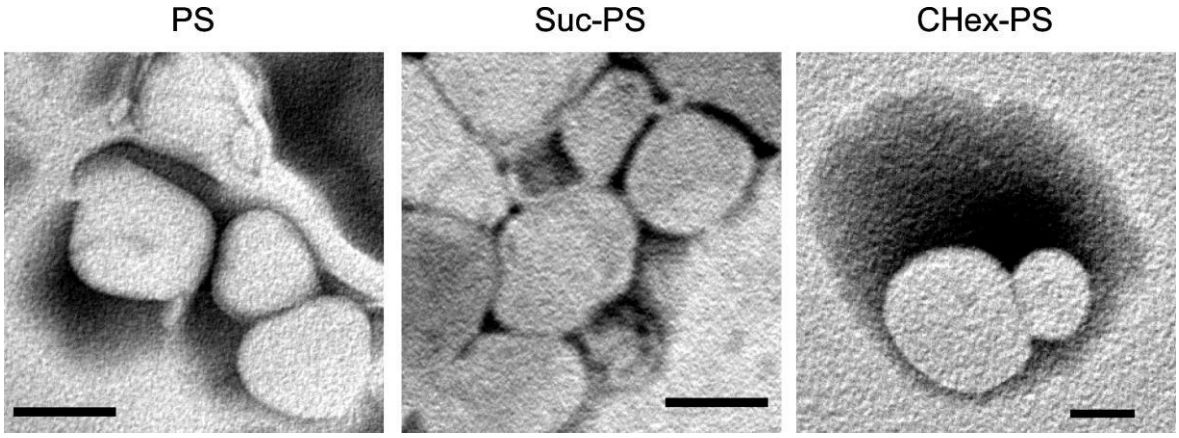

Figure 3. TEM images of liposomes composed of DMPC and phytosterol derivatives. Scale bars represent 100 nm.

Table 1. Size of Liposome

Liposome	Size (nm)	Polydispersity index
PS[1]	105.7 ± 1.3	0.20 ± 0.03
Suc-PS[2]	103.8 ± 1.4	0.08 ± 0.02
CHex-PS[3]	104.5 ± 0.8	0.11 ± 0.05

[1]n = 5, [2]n = 2, [3]n = 8.

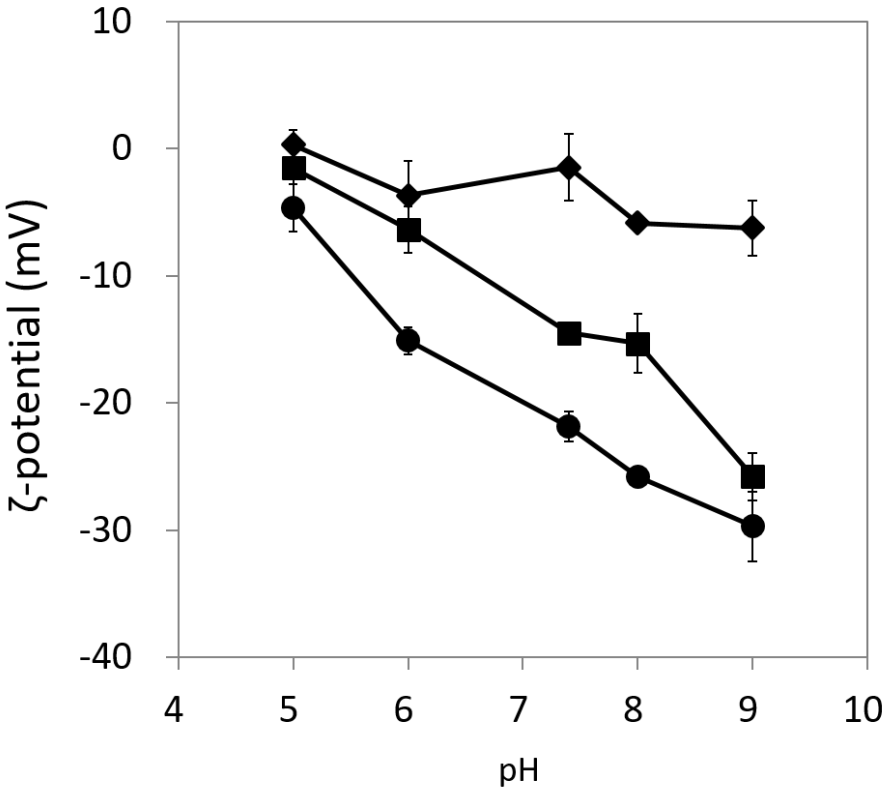

Figure 4. pH dependence of zeta potentials of liposomes containing PS (diamonds), Suc-PS (circles) and CHex-PS (squares).

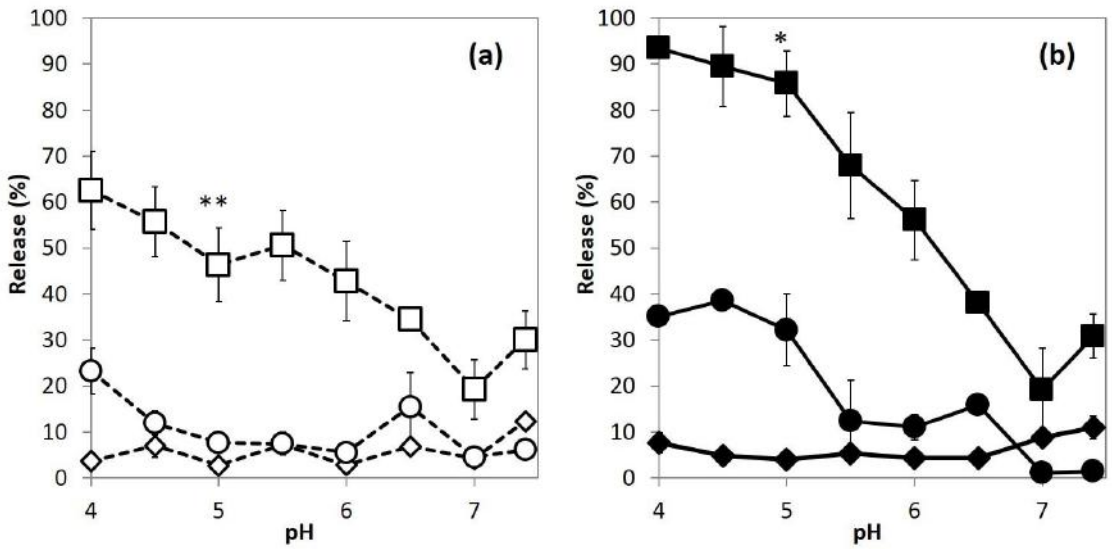

Figure 5. pH dependence of calcein release after 30 min-incubation from liposomes containing PS (diamonds), Suc-PS (circles) and CHex-PS (squares) at 25°C (a) or 35°C (b). * $p < 0.05$ and ** $p < 0.01$ for other groups.

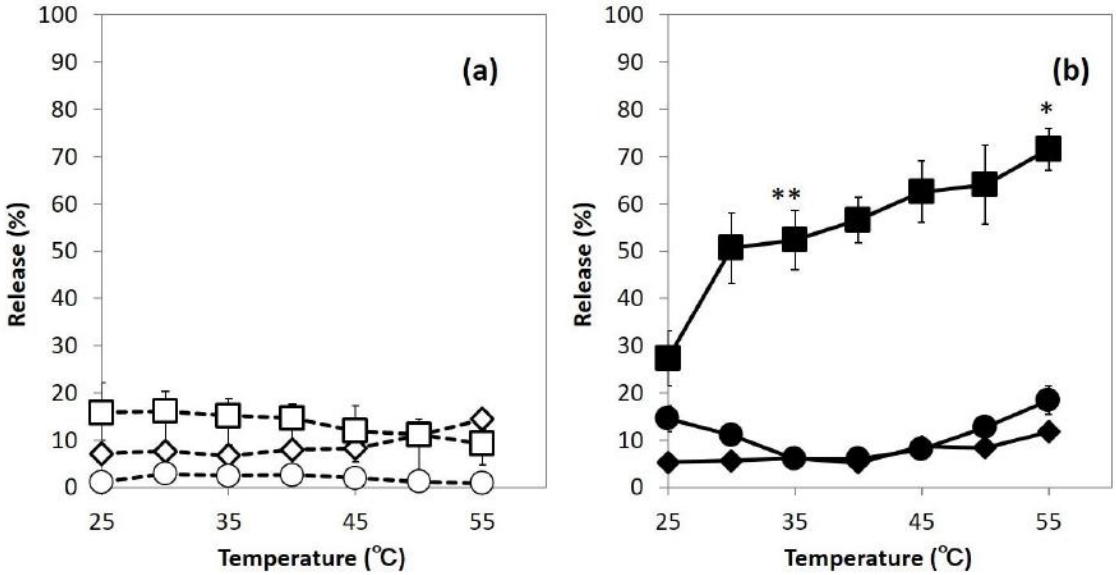

Figure 6. Temperature dependence of calcein release after 10 min-incubation from liposomes containing PS (diamonds), Suc-PS (circles) and CHex-PS (squares) at pH 7.4 (a) or 5.0 (b). * $p < 0.05$ and ** $p < 0.01$ for other groups.

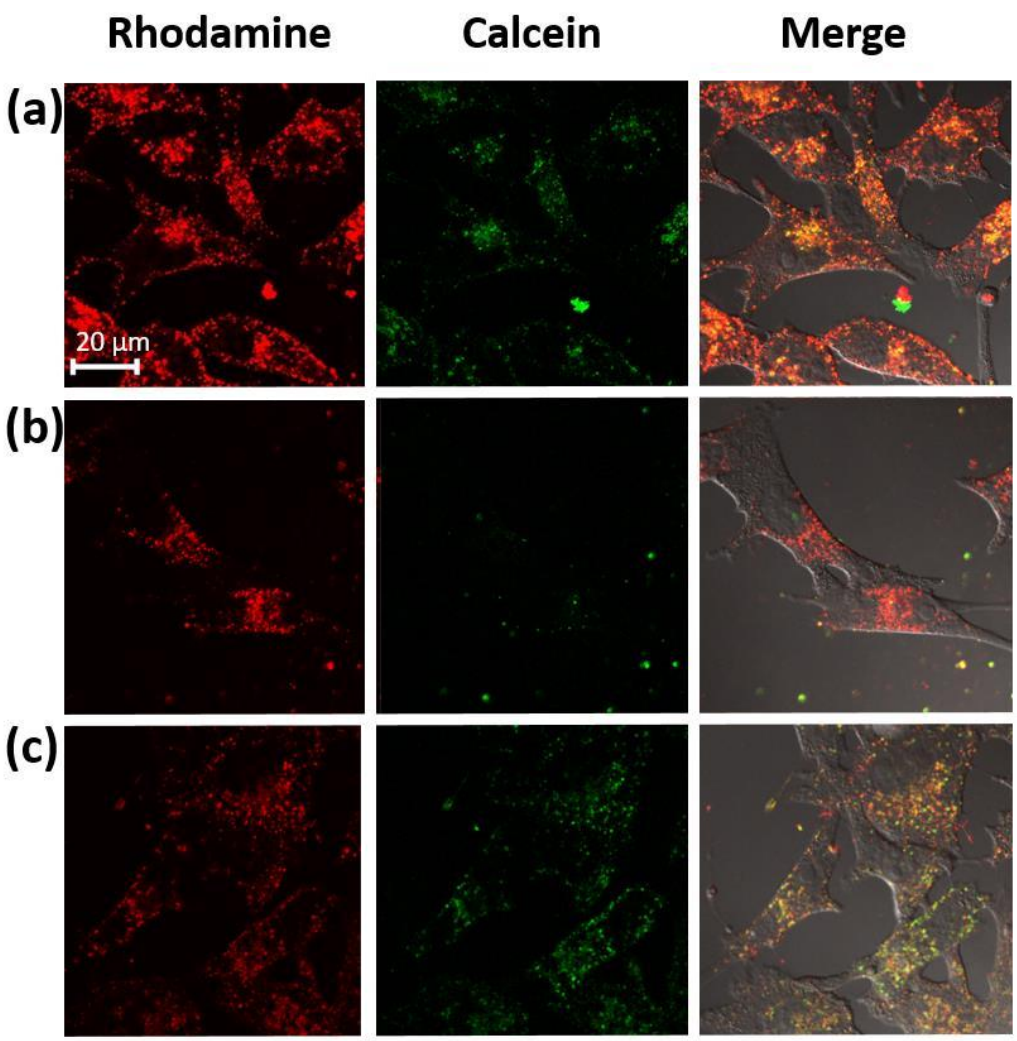

Figure 7. Confocal laser scanning microscopic (CLSM) images of B16-F10 melanoma cells treated with calcein-loaded, rhodamine-lipid-labeled liposomes containing PS (a), Suc-PS (b), and CHex-PS (c) for 3 h. Scale bar represents 10 μm.

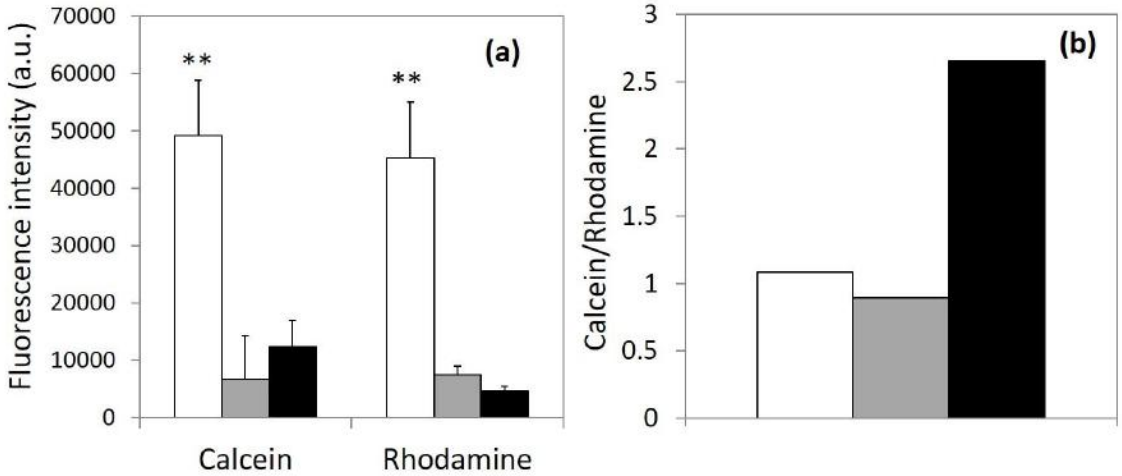

Figure 8. (a) Fluorescence intensity for B16-F10 melanoma cells treated with calcein-loaded, Rh-PE-lipid-labeled liposomes containing PS (open bars), Suc-PS (gray bars), and CHex-PS (closed bars) for 3 h. ** $p < 0.01$ for other groups. (b) Ratio of fluorescence intensity of calcein/Rh.

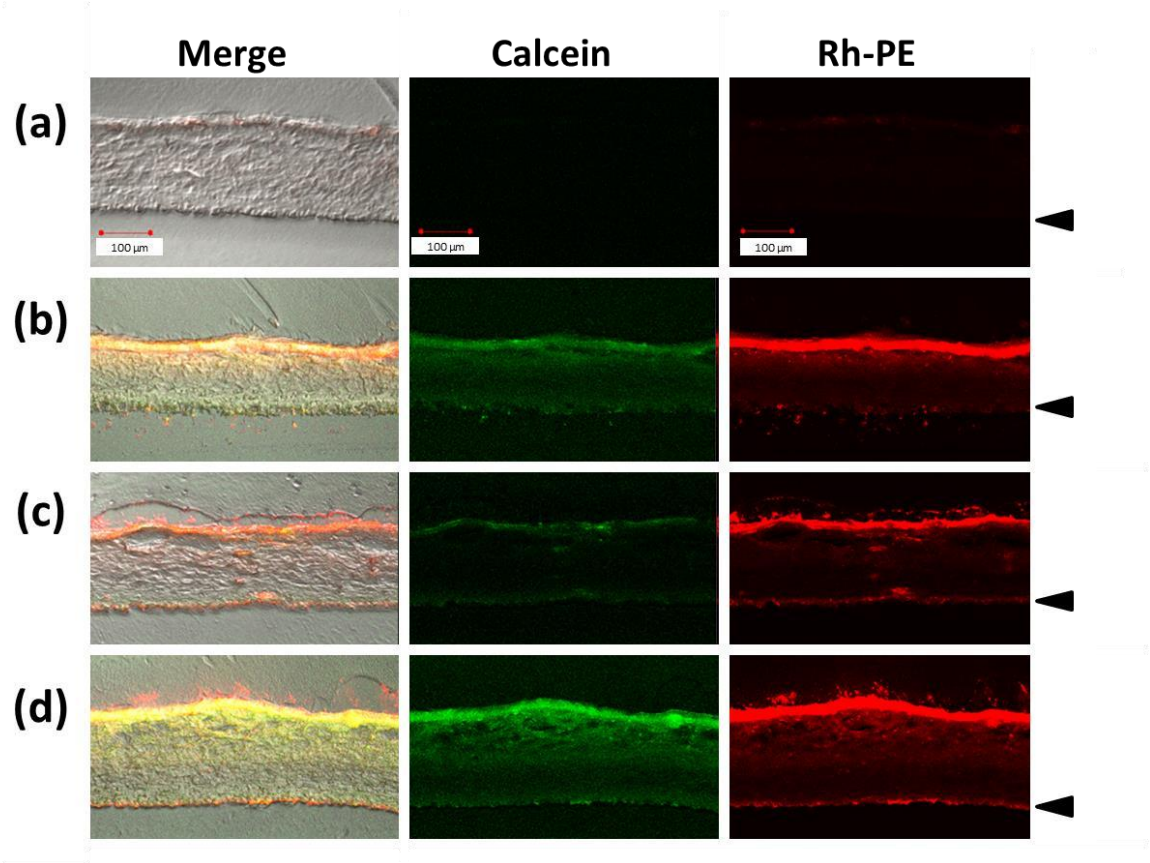

Figure 9. CLSM images of 3D skin model treated with PBS (a), calcein-loaded, Rh-PE-labeled liposomes containing PS (b), Suc-PS (c) and CHex-PS (d) for 24 h. Arrowheads indicate the basement membrane.

Supporting Information

Carboxylated phytosterol derivative-introduced liposomes for skin environment-responsive transdermal drug delivery system

Naoko Yamazaki[a,b], Satoshi Yamakawa[c], Takumi Sugimoto[b], Yuta Yoshizaki[b], Ryoma Teranishi[b], Takaaki Hayashi[b], Aki Kotaka[a], Chiharu Shinde[a], Takayuki Kumei[a], Yasushi Sumida[a], Toru Shimizu[c], Yukihiro Ohashi[c], Eiji Yuba[b,*], Atsushi Harada[b], and Kenji Kono[b]

[a] *Research Institute, Fancl Corporation, 12-13 Kamishinano, Totsuka-ku, Yokohama, Kanagawa, Japan*

[b] *Department of Applied Chemistry, Graduate School of Engineering, Osaka Prefecture University, 1-1 Gakuen-cho, Naka-ku, Sakai, Osaka 599-8531, Japan*

[c] *Cosmetic Ingredients Laboratory, Nippon Fine Chemical Corporation, 1-1, 5-Chome, Umei, Takasago, Hyogo 676-0074, Japan*

***Corresponding author: Eiji Yuba**

Department of Applied Chemistry, Graduate School of Engineering,

Osaka Prefecture University, 1-1 Gakuen-cho, Naka-ku, Sakai, Osaka 599-8531, Japan

Tel.: +81-722-54-9913; Fax: +81-722-54-9330; yuba@chem.osakafu-u.ac.jp

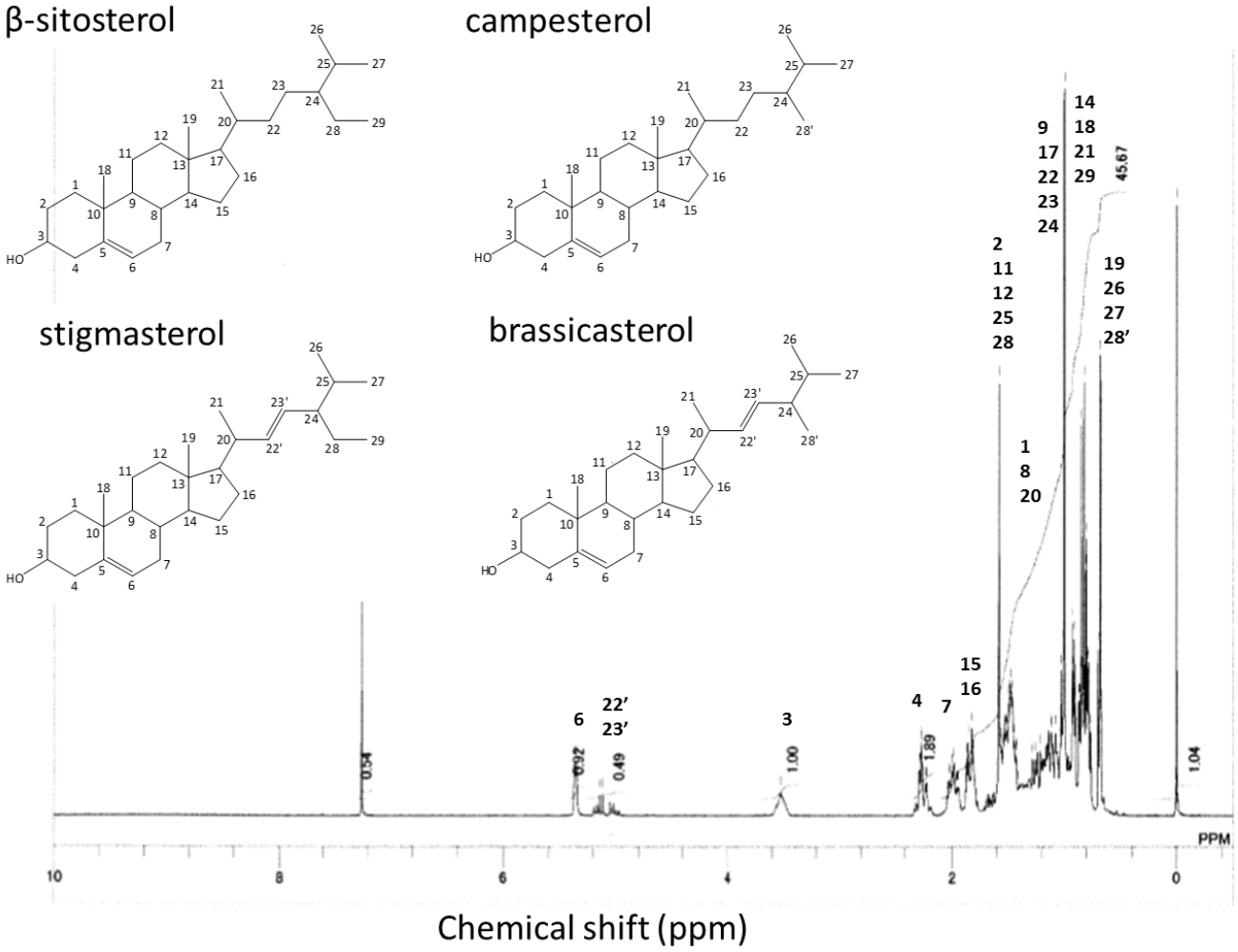

Fig. S1. ^{1}H NMR spectrum of phytosterol (300 MHz, $CDCl_3$).

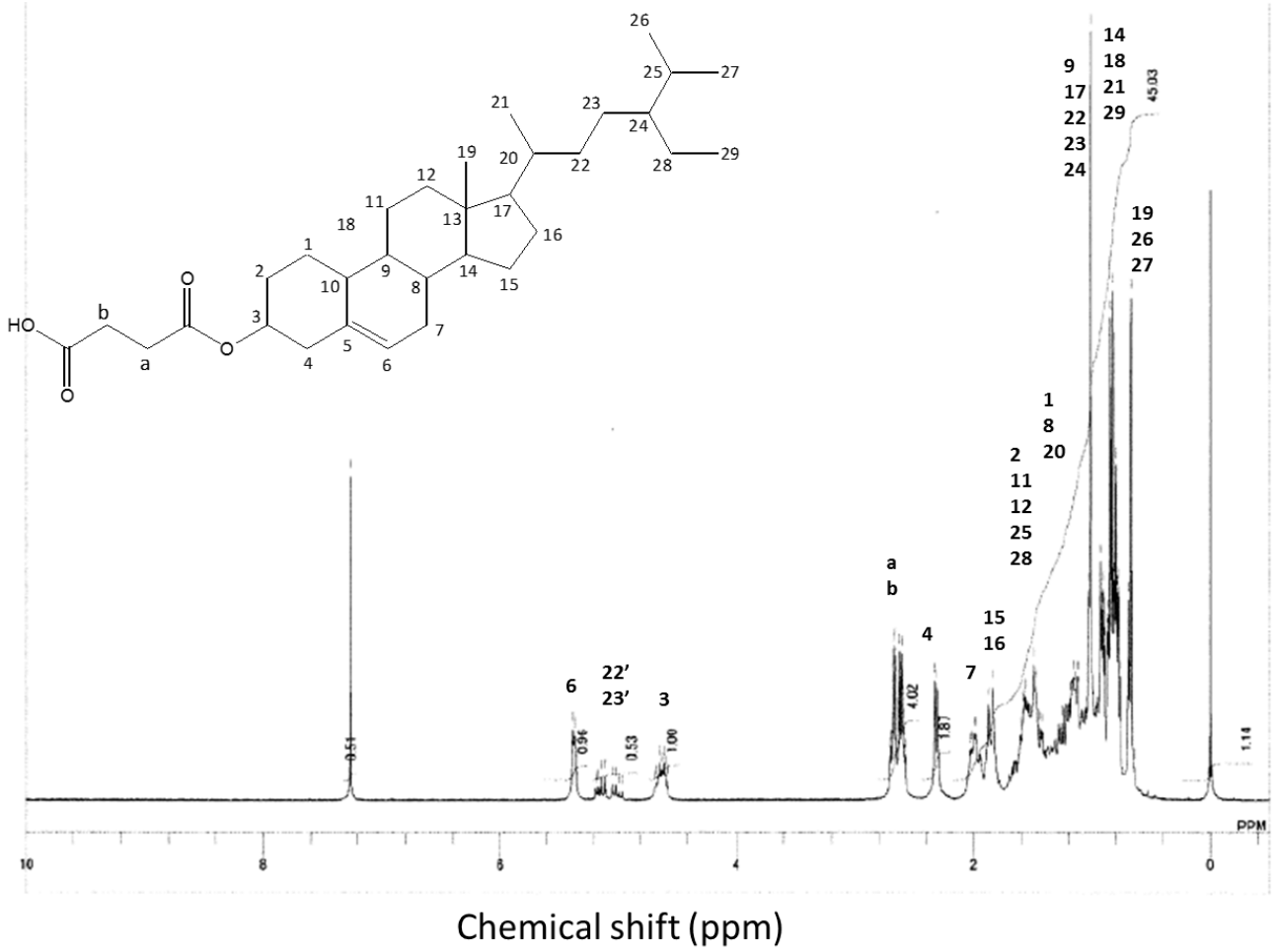

Fig. S2. ^{1}H NMR spectrum of Suc-phytosterol (300 MHz, $CDCl_3$).

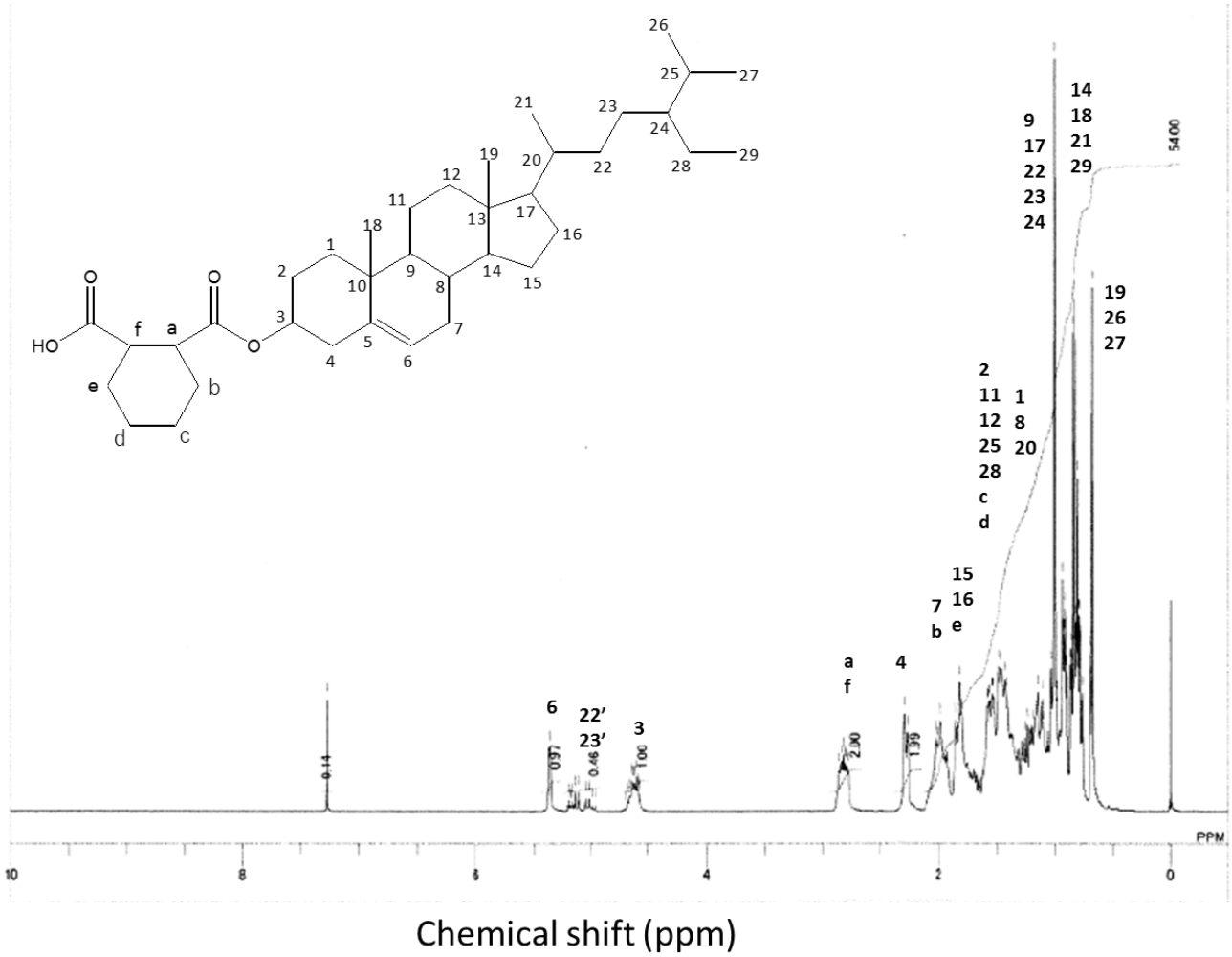

Fig. S3. ^{1}H NMR spectrum of CHex-phytosterol (300 MHz, $CDCl_3$).

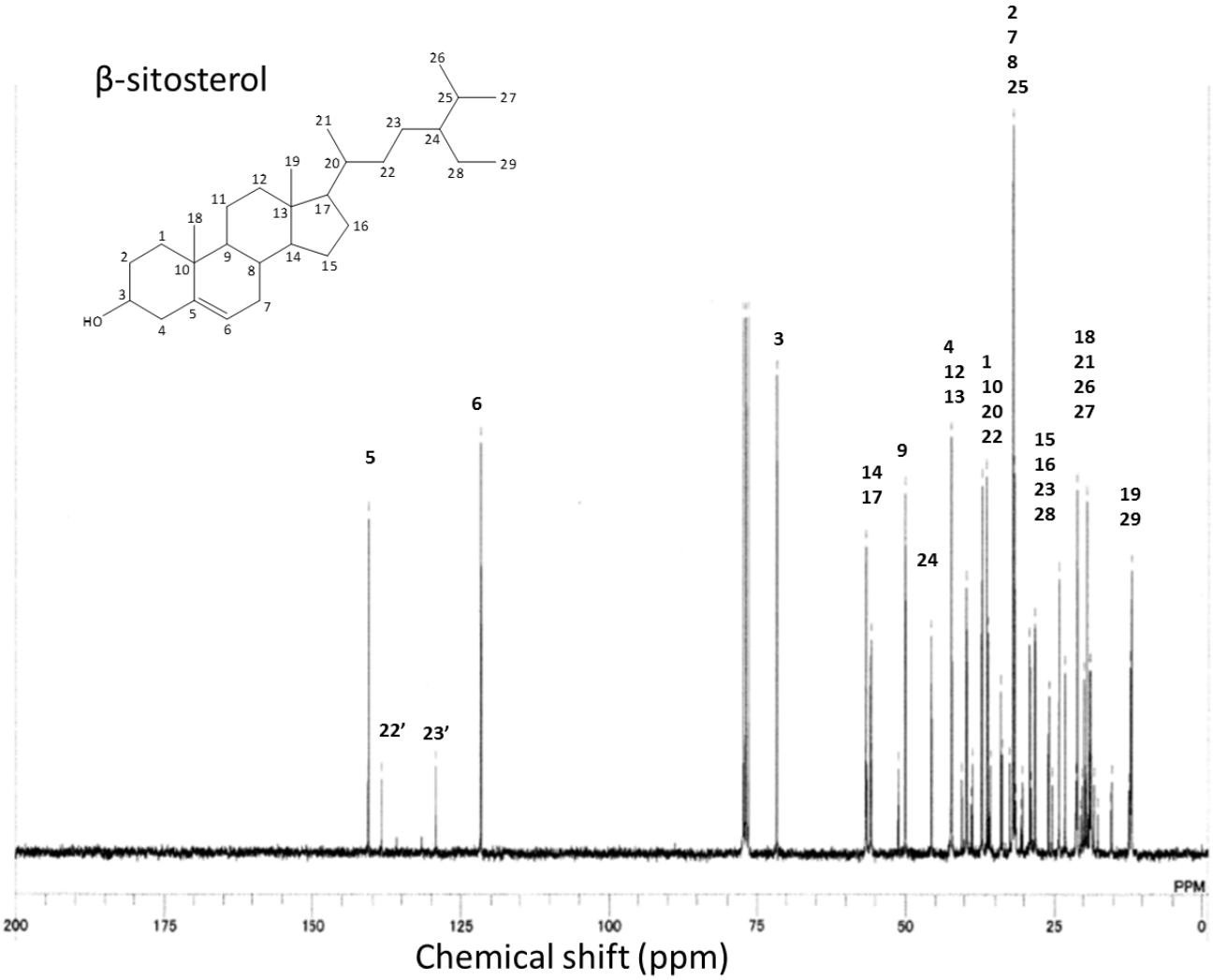

Fig. S4. ^{13}C NMR spectrum of Phytosterol (75.45 MHz, $CDCl_3$).

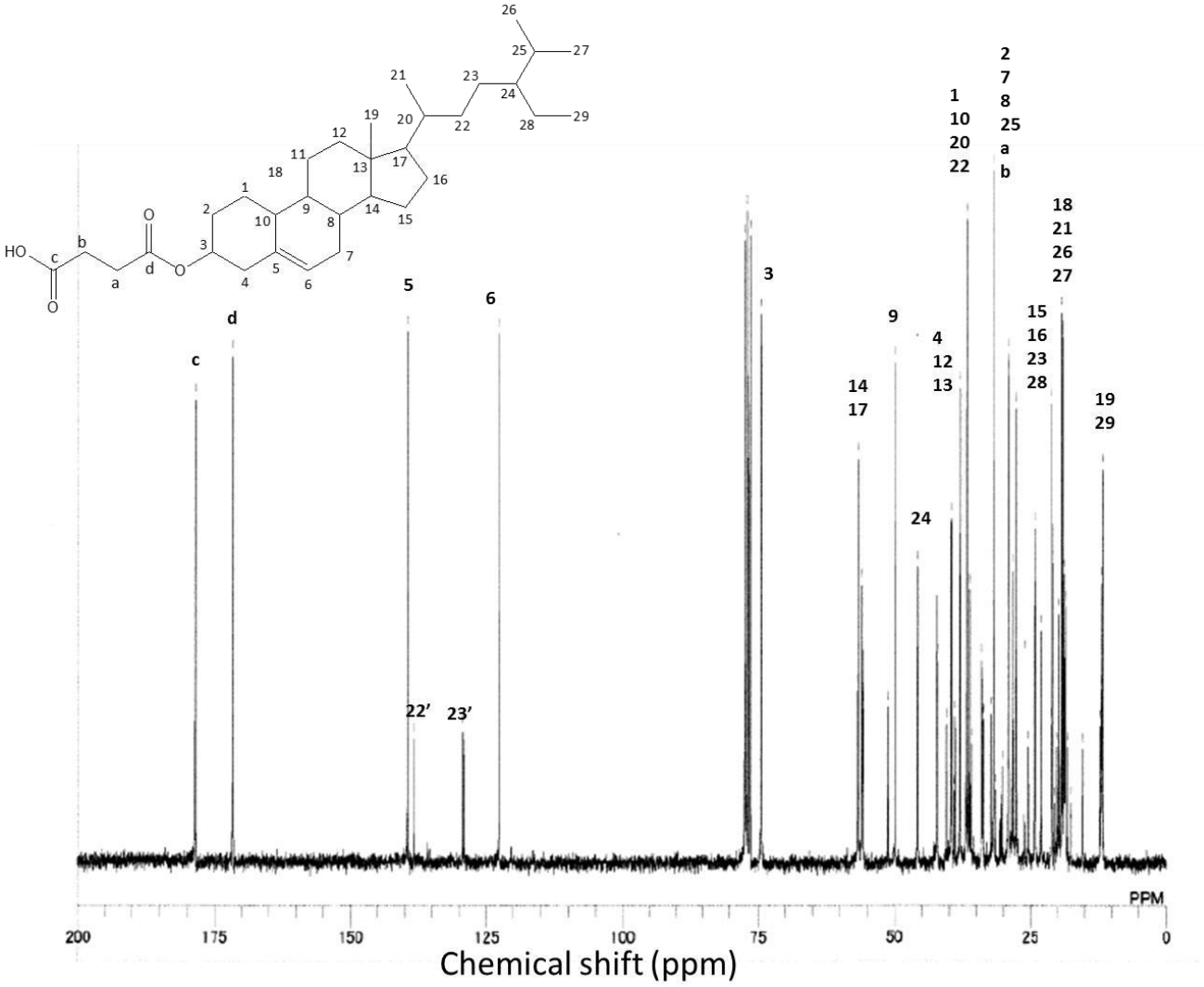

Fig. S5. ^{13}C NMR spectrum of Suc-phytosterol (75.45 MHz, $CDCl_3$).

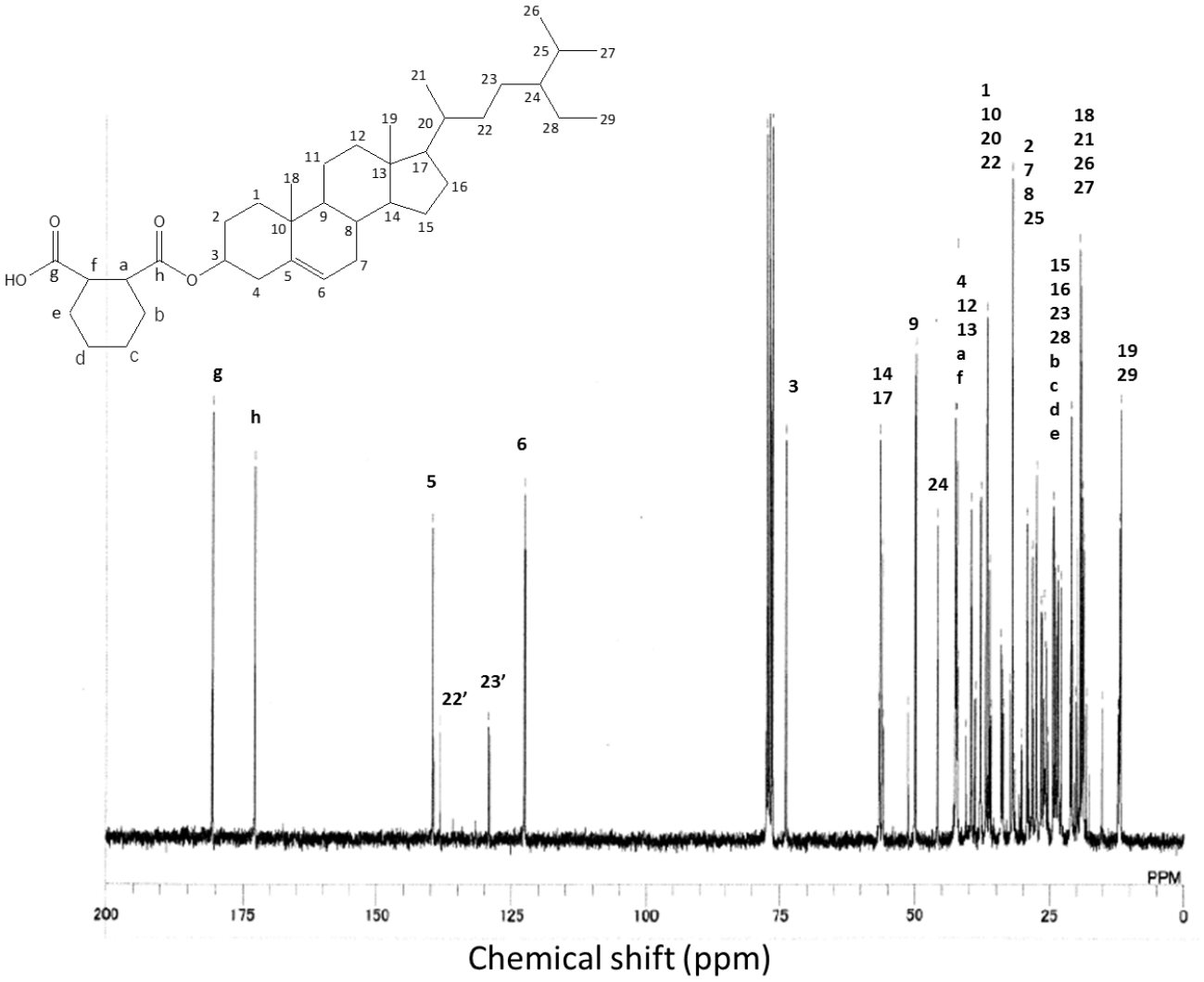

Fig. S6. ^{13}C NMR spectrum of CHex-phytosterol (75.45 MHz, $CDCl_3$).

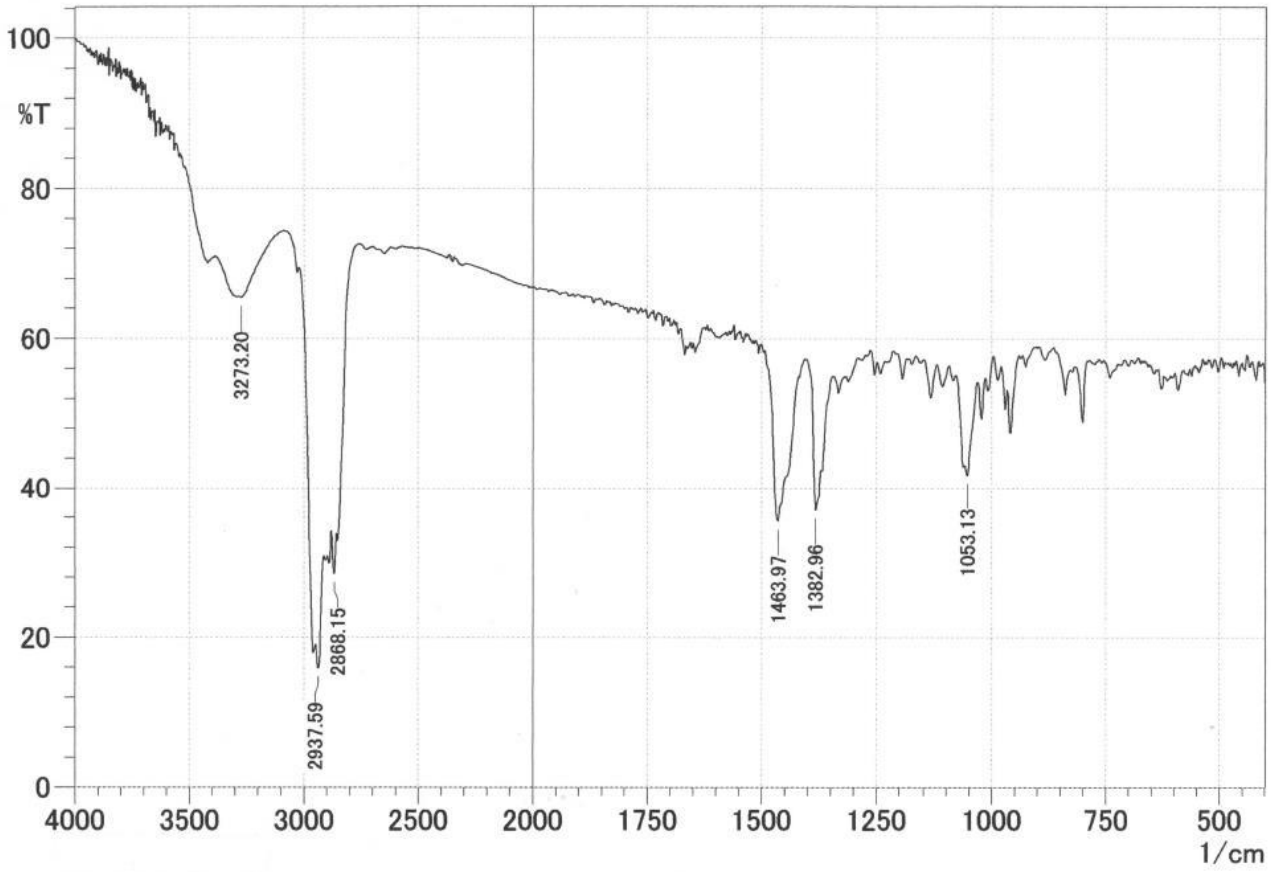

Fig. S7. IR spectrum of phytosterol. 1382 cm^{-1}: $\delta(CH_3)$, 1462 cm^{-1}: $\delta_{as}(CH_2, CH_3)$, 2868/2953 cm^{-1}: ν_{s+as} (CH_2, CH_3), 3273 cm^{-1}: $\nu(OH)$. ν, stretching mode; δ, bending in plane; s, symmetric vibration; as, asymmetric vibration.

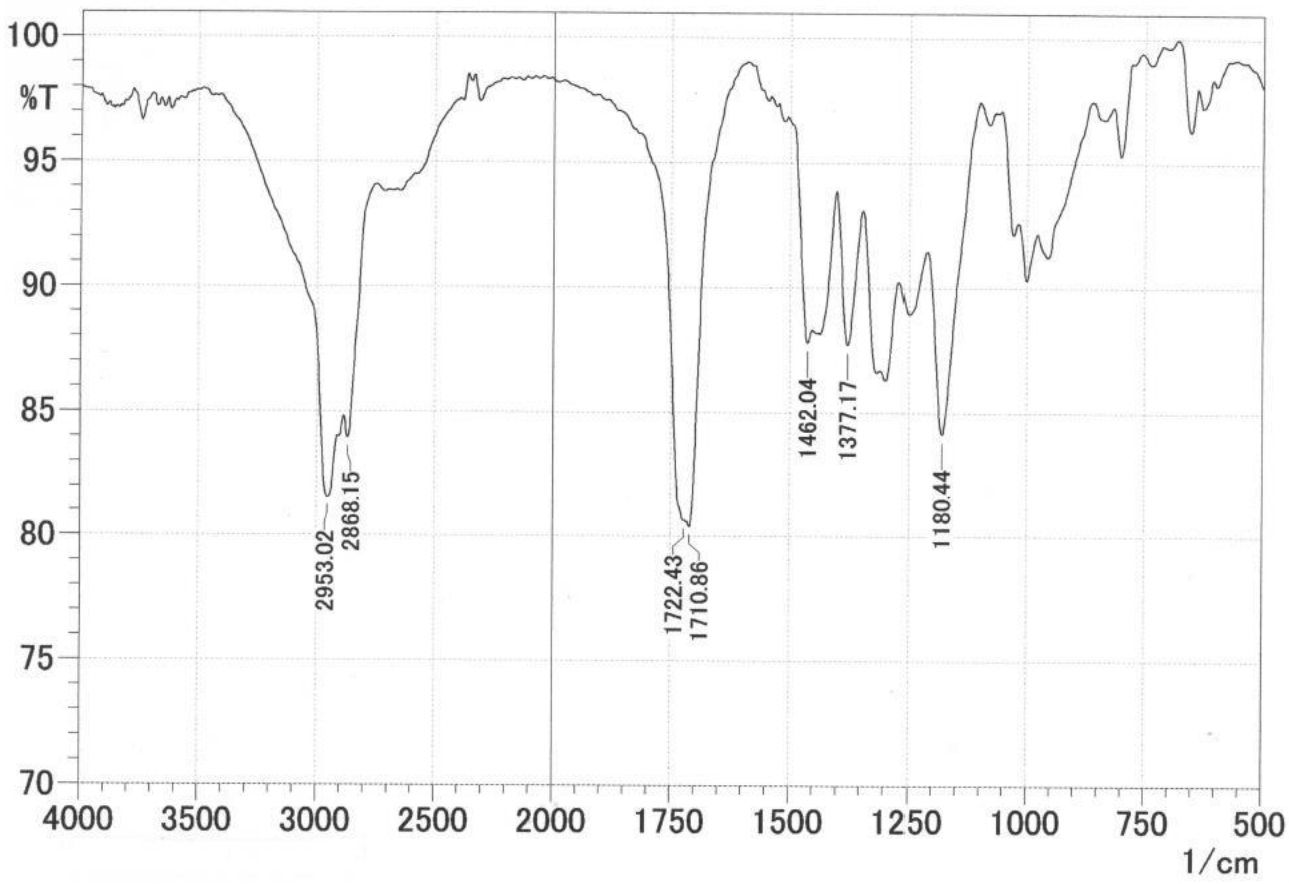

Fig. S8. IR spectrum of Suc-phytosterol. 1180 cm^{-1}: ν(C-O-C) for ester, 1377 cm^{-1}: $\delta(CH_3)$, 1462 cm^{-1}: $\delta_{as}(CH_2, CH_3)$, 1710/1722 cm^{-1}: $\nu_{as}(C=O)$ for ester, 2868/2953 cm^{-1}: ν_{s+as} (CH_2, CH_3). ν, stretching mode; δ, bending in plane; s, symmetric vibration; as, asymmetric vibration.

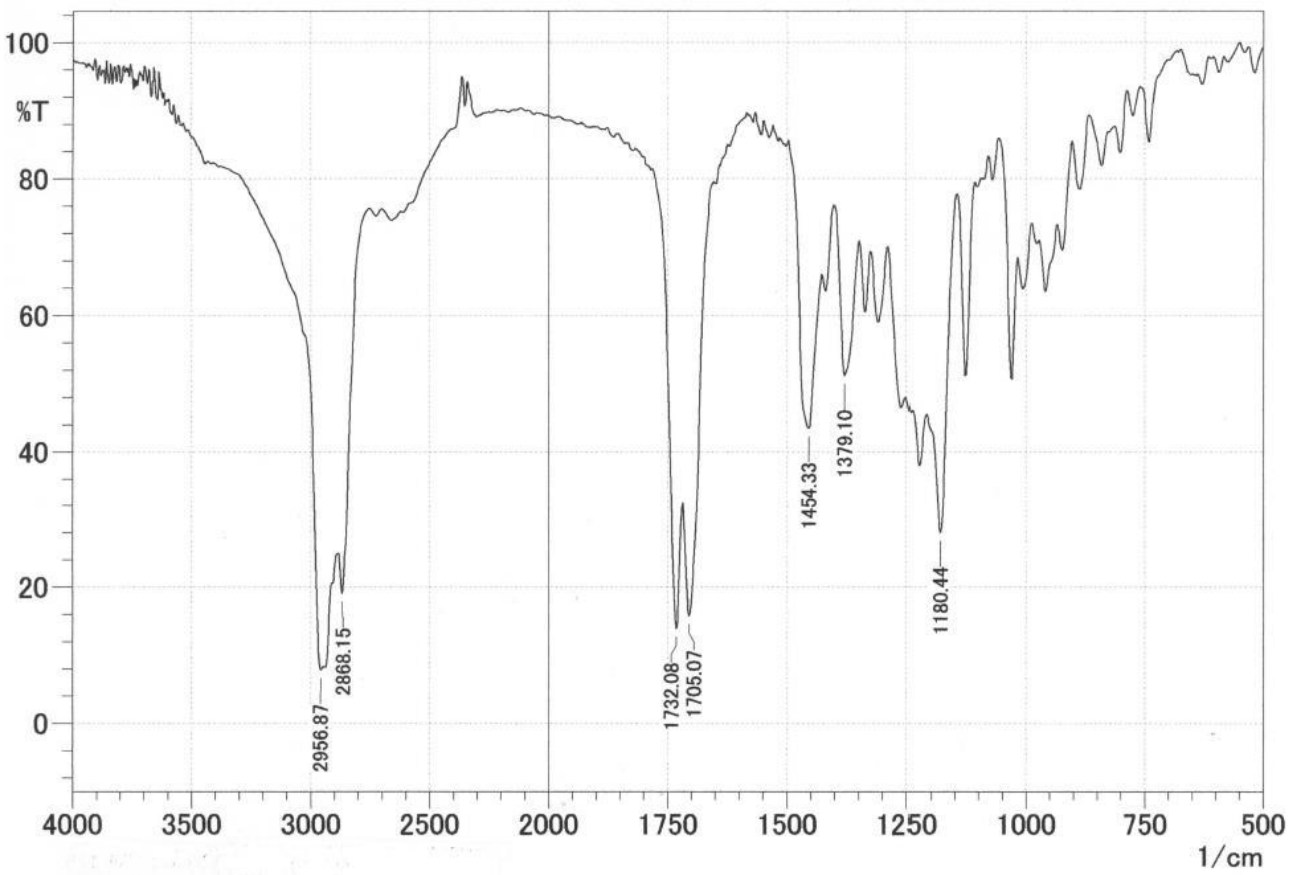

Fig. S9. IR spectrum of CHex-phytosterol. 1180 cm^{-1}: ν(C-O-C) for ester, 1379 cm^{-1}: $\delta(CH_3)$, 1454 cm^{-1}: $\delta_{as}(CH_2, CH_3)$, 1705/1732 cm^{-1}: $\nu_{as}(C=O)$ for ester, 2868/2958 cm^{-1}: ν_{s+as} (CH_2, CH_3). ν, stretching mode; δ, bending in plane; s, symmetric vibration; as, asymmetric vibration.

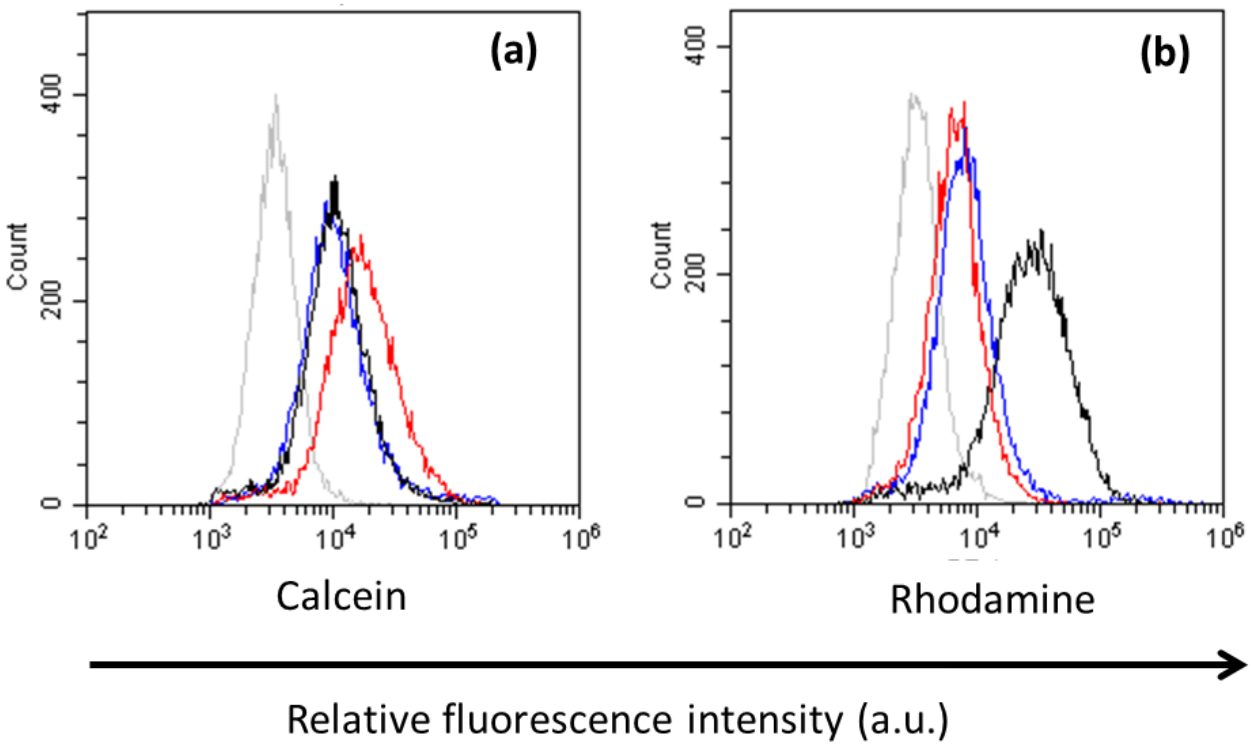

Fig. S10. Histograms of calcein (a) or rhodamine (b) fluorescence intensity for cells treated with calcein-loaded, Rh-PE-lipid-labeled liposomes containing PS (black lines), Suc-PS (blue lines), and CHex-PS (red lines) for 3 h. Fluorescence intensity for untreated cells (gray line) was also shown as a negative control.